IPM/P-2010/029

Orientifolded Locally AdS_3 Geometries

F. Loran[1] and M. M. Sheikh-Jabbari[2]

[1] *Department of Physics, Isfahan University of Technology, Isfahan 84156-83111, Iran*

[2] *School of Physics, Institute for research in fundamental sciences (IPM), P.O.Box 19395-5531, Tehran, Iran*

E-mail: loran@cc.iut.ac.ir, jabbari@theory.ipm.ac.ir

Abstract

Continuing the analysis of [arXiv:1003.4089[hep-th]], we classify all locally AdS_3 stationary axi-symmetric *unorientable* solutions to AdS_3 Einstein gravity and show that they are obtained by applying certain orientifold projection on AdS_3, BTZ or AdS_3 self-dual orbifold, respectively O-AdS_3, O-BTZ and O-SDO geometries. Depending on the orientifold fixed surface, the O-surface, which is either a space-like $2D$ plane or cylinder, or a light-like $2D$ plane or cylinder one can distinguish four distinct cases. For the space-like orientifold plane or cylinder cases these geometries solve AdS_3 Einstein equations and are hence locally AdS_3 everywhere except at the O-surface, where there is a delta-function source. For the light-like cases the geometry is a solution to Einstein equations even at the O-surface. We discuss the causal structure for static, extremal and general rotating O-BTZ and O-SDO cases as well as the geodesic motion on these geometries. We also discuss orientifolding Poincaré patch AdS_3 and AdS_2 geometries as a way to geodesic completion of these spaces and comment on the $2D$ CFT dual to the O-geometries.

Contents

1 Introduction

Three dimensional gravity, due to its relative simplicity compared to higher dimensional gravity theories, has been used as a laboratory to address questions about quantum gravity. Three dimensional Einstein gravity on the flat space background has neither propagating gravitons nor nontrivial (black hole) classical solutions, its partition function has been computed noting that this theory is in fact an SL(2, R) Chern-Simons theory [1]. Addition of a negative cosmological constant to the theory brings the possibility of having black hole solutions, the BTZ black holes [2, 3]. BTZ black holes has appeared as the prime arena for

addressing black hole thermodynamics puzzles and seeking statistical mechanical resolutions in terms of the proposed dual $2D$ CFT.

In three dimensions Riemann tensor is completely specified by the Ricci tensor [4] and as such Einstein equations imply that all the solutions to the pure AdS_3 Einstein gravity should be locally AdS_3. Therefore, the only option for solutions other than (global) AdS_3 geometry is to orbifold AdS_3 by a subgroup of its $O(2,2)$ isometry group. And for the latter, as we will review briefly in section 2 and discussed in [2, 3, 5], besides the trivial (space-like) AdS_3 orbifolds $AdS_3/\mathbb{Z}_k$ there seems to be only two possibilities leading to either BTZ black hole or the AdS_3 self-dual-orbifold (SDO). (We are of course excluding the pathologic geometries which involve closed time-like curves, CTC's, not dressed by an event horizon.)

In [6] we revisited the problem of classification of solutions to AdS_3 gravity and noted that AdS_3 geometry besides the orientation preserving $SO(2,2)$ isometry is invariant under an orientation changing $\mathbb{Z}_2$ and one may construct a new class of solutions by orbifolding (orientifolding) this $\mathbb{Z}_2$. In this way we constructed the new class of BTZ geometries, *orientifold-BTZ* or O-BTZ geometries. There are various possibilities for the choice of this $\mathbb{Z}_2$ but there is only one possibility which does not change the orientation on the $2D$ causal (conformal) boundary of the AdS_3. This $\mathbb{Z}_2$ commutes with the BTZ orbifolding and hence the orientifolding and BTZ orbifolding can be performed at the same time.

In this work we extend the analysis of [6] and construct all the orientifold AdS_3 geometries, *O-geometries* for short, with this choice of $\mathbb{Z}_2$. As we will show the O-geometries are necessarily of the form of orientifolded AdS_3 (O-AdS_3), orientifolded BTZ (O-BTZ) or orientifolded self-dual-AdS_3-orbifold (O-SDO). These O-geometries, are hence locally AdS_3 by construction. There is, however, a special locus, the *O-surface*, the fixed $2D$ surface of the orientifold operation we perform. The O-surface, being fixed point of the orientifold projection, should in fact be viewed as the boundary (of course not a conformal, causal boundary) of the O-geometries. The O-surface is in fact a Cauchy surface. As we will explicitly show this orientifold fixed locus is a $2D$ space-like surface with topology of R^2 for the case of O-AdS_3 while it is a cylinder for generic O-BTZ. This space-like fixed plane (cylinder) becomes light-like when we approach the causal boundary of the geometry. For extremal O-BTZ the O-surface is light-like. For the O-SDO there are two possibilities of having space-like or light-like $2D$ fixed cylinders.

As discussed O-geometries are locally AdS_3 everywhere away from the O-surface. One may still study the curvature of the O-geometry at the O-surface which should be viewed as the "end locus" of the geometry. This may be carried out if we go to the "covering space" of the projection and extend the space to behind the O-surface. One may then use the Israel matching conditions [7] or its refined formulation of [8] (which is reviewed in Appendix C) to compute the Ricci at the O-surface. The Ricci, which as we will show has a delta-function jump at the O-surface, may be associated to a stress tensor of an "orientifold plane" (cylinder) sitting at the O-surface. We note, however, that for the light-like O-surface the Ricci is continuous.

In this paper we study in some detail the orientifolded locally AdS_3 geometries as classical (Einstein) gravity backgrounds. In section 2 we review the known and well-established

solutions to pure AdS_3 Einstein gravity. We review construction of BTZ and self-dual AdS_3 orbifold solutions. In section 3 we argue for the possibility of constructing locally AdS_3 *unoriented* geometries (O-geometries), classify all of them and analyze their causal structure. In section 4 we study geodesic motion on the O-geometries. In the last section, the discussion section, we discuss the relevance of the O-BTZ geometries to the possible dual $2D$ CFT description for the AdS_3 Einstein quantum gravity and outline future studies in this direction. In a couple of appendices we have gathered a summary of useful notations, some technical details of the computations and some new solutions to AdS_3 Einstein gravity coupled to conformal matter fields.

2 Orientable solutions to AdS_3 Einstein gravity, a quick review

As mentioned in the introduction all the solutions of AdS_3 Einstein gravity are locally AdS_3 and may be obtained by modding out the space by a subgroup of its isometries. In this section we review the well-known solutions, namely BTZ black holes and the self-dual AdS_3 orbifold (SDO) which are obtained by modding out the AdS_3 space by a part of its orientation preserving $SO(2,2)$ isometry group.

2.1 The BTZ black holes

A generic rotating BTZ black hole can be constructed by orbifolding original AdS_3 by the boosts of its $SO(2,2)$ isometry. In terms of the embedding space coordinates (A.1) that is,

$$\begin{aligned} T_1 \pm X_1 &\equiv e^{\pm \frac{2\pi r_+}{\ell}} (T_1 \pm X_1) \ , \\ T_2 \pm X_2 &\equiv e^{\pm \frac{2\pi r_-}{\ell}} (T_2 \pm X_2) \ . \end{aligned} \tag{2.1}$$

where $r_+ > r_- \geq 0$. $r_+ = r_-$ case, corresponding to the extremal (or massless for $r_+ = r_- = 0$) BTZ black hole is in a different class and cannot be constructed through (2.1). For $r_- = 0$, the static BTZ black hole, the above orbifolding has a fixed line at $T_1 = X_1 = 0$, $T_2^2 - X_2^2 = \ell^2$ while for generic $r_- \neq 0$ case the orbifolding is freely acting on AdS_3 and we have a smooth geometry. In the coordinate system (A.13) the BTZ identification (2.1) is written as

$$(\tilde{\tau}, \tilde{r}, \tilde{\phi}) \sim (\tilde{\tau} - 2\pi r_-/\ell, \ \tilde{r}, \ \tilde{\phi} + 2\pi r_+/\ell). \tag{2.2}$$

The BTZ geometry has two horizons which in our coordinate system (A.13) are at $\tilde{r} = \ell$ and $\tilde{r} = 0$. In the BTZ coordinates (when $r_+ \neq r_-$)

$$\begin{aligned} \tilde{\tau} &= \tfrac{1}{\ell}(r_+ \tau - r_- \phi), \\ \tilde{\phi} &= \tfrac{1}{\ell}(r_+ \phi - r_- \tau), \\ \tilde{r}^2 &= \tfrac{\ell^2}{r_+^2 - r_-^2}(r^2 - r_-^2), \end{aligned} \tag{2.3}$$

metric takes the form

$$ds^2 = \rho^2 d\tau^2 + \frac{r^2 dr^2}{16G^2J^2 - \frac{r^2\rho^2}{\ell^2}} + r^2 d\phi^2 - 8G\ell J d\tau d\phi, \tag{2.4}$$

where now the identification is only made along the ϕ coordinate $\phi \in [0, 2\pi]$ and

$$\rho^2 = 8GM\ell^2 - r^2. \tag{2.5}$$

In this coordinate system the outer and inner horizons are located at $r = r_+$ and $r = r_-$ respectively. The (ADM) mass M and angular momentum J are given by

$$M = \frac{r_+^2 + r_-^2}{8\ell^2 G}, \quad J = \frac{r_+ r_-}{4G\ell}\ . \tag{2.6}$$

We note that the coordinate transformation (2.3) is singular for the extremal $r_+ = r_-$ case. As discussed in [3], however, one may still use (2.4) for this case.

As discussed in [2, 3] the identification (2.2) leads to closed time-like curves (CTC's). Recalling metric (A.9), the CTC's will be generated where

$$\mathcal{D} = -(\tilde{r}^2 - \ell^2)r_-^2 + \tilde{r}^2 r_+^2 = \tilde{r}^2(r_+^2 - r_-^2) + \ell^2 r_-^2 \tag{2.7}$$

which measures the length of the curve closed by the identifications, becomes negative. With our choice $r_+ > r_- \geq 0$ CTC's develop for

$$\tilde{r}^2 \leq \tilde{r}^2_{CTC} = -\ell^2 \frac{r_-^2}{r_+^2 - r_-^2} < 0. \tag{2.8}$$

That is, in region III (*cf.* Appendix A) we will have CTC's. In the BTZ coordinates (2.3) this happens at $r^2 < 0$ ($\rho^2 > 8GM\ell^2$). To remove inconsistencies arising from CTC's, as prescribed in [3], the $r^2 < 0$ region is cut out from the geometry.[1] This would render the BTZ black hole geometry as geodesically incomplete. Although region III is not accessible to any observer from region I, points in region III and II can be related by geodesics. This renders the BTZ black holes as geodesically incomplete and may cause problems for a quantum gravity description of BTZ geometries (e.g. using dual CFT language). Despite the arguments for the necessity of excising the inner horizon and the region behind it from the geometry (e.g. see [12, 13]) it is not clear whether it is possible to carry this out within a (unitary) dual CFT. Penrose diagram of the BTZ geometry is depicted in Fig.1.

[1] It was argued in [3] that for the static case addition of any matter to the BTZ background turns $r = 0$ to a curvature singularity. This latter was confirmed in [9, 10] by showing that expectation value of the energy momentum tensor corresponding to quantum fluctuations of a matter field added on the BTZ background blows up at $r = 0$, a result which is also supported by semi-classical AdS/CFT treatments using (space-like) geodesics [11, 12]. One can then show explicitly that the back-reaction of this energy momentum tensor on the geometry creates a curvature singularity at $r = 0$ (see Appendix B). For the $J \neq 0$ rotating backgrounds, however, the situation is different. The energy momentum corresponding to fluctuations of any matter field will blow up at the inner horizon $r = r_-$, rather than $r = 0$. This result agrees with semiclassical AdS/CFT analysis based on (space-like) geodesics [13]. However, back-reaction of energy momentum tensor given in [9, 10] seems to destroy the asymptotic AdS_3 geometry, making the perturbative analysis of [9, 10], where the back-reaction effects are not accounted for, inapplicable.

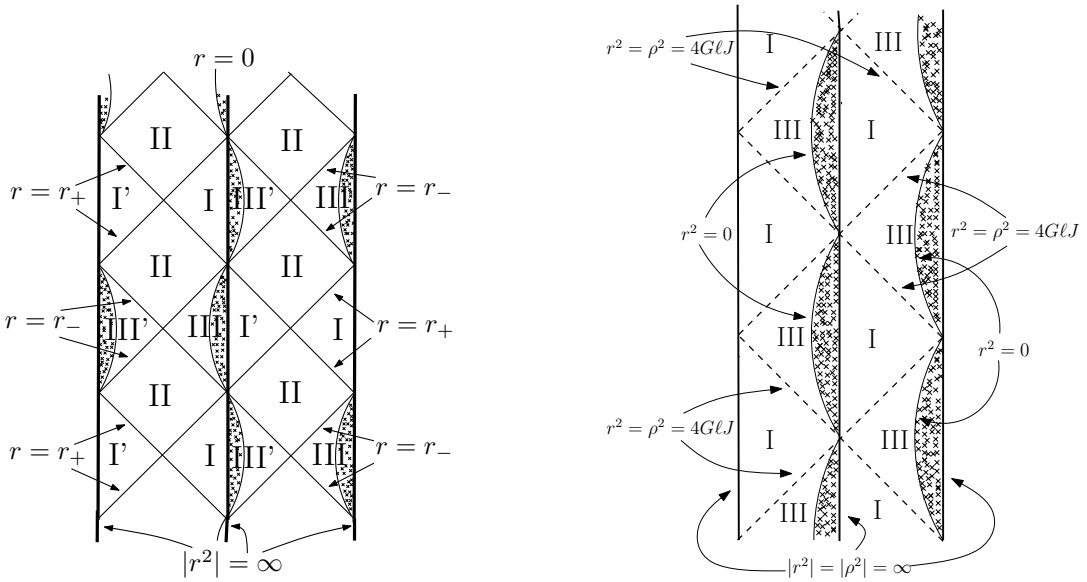

Figure 1: *Two Penrose diagrams of BTZ black holes drawn side-by-side.* ***Left figure****: A generic rotating BTZ.* Regions I, I' are bounded between the boundary at $r^2 = +\infty$ and the outer horizon at $r = r_+$. Region II is the region between the two horizons and Regions III, III' are bounded between the inner horizon (which is also a Cauchy horizon) and boundary at $\rho^2 = \infty$. ***Right figure****: An extremal BTZ.* Here the region II is absent and the two horizons coincide. The horizon in this case is also a Cauchy horizon. In both of the cases Region III may not be reached by any physical observer from the Region I and the hatched area, corresponding to $r^2 < 0$, which is the region containing closed time-like curves, is cut from the BTZ geometry. As depicted, this region contains a part of the causal boundary of original AdS_3 [3]. In the figure ϕ direction has been suppressed and the $|r^2| = \infty$ lines correspond to $\phi = 0, \pi, 2\pi$. To convey the idea of the suppressed ϕ direction and that r coordinate can be extended past $r^2 < 0$ we have drawn two Penrose diagrams side-by-side.

2.2 The AdS_3 self-dual-orbifold, SDO

BTZ geometries are stationary, axisymmetric, asymptotically AdS_3 black hole solutions of pure Einstein AdS_3 gravity. There is another solution of this theory, which is not a black hole and preserves SL(2,R)×U(1) of the $SO(2,2)$ isometry and similarly to the BTZ case can be obtained through orbifolding AdS_3 by the appropriate element of the $SO(2,2)$ isometry group. These are the so-called AdS_3 self-dual orbifold (SDO) geometries constructed in [5], see also [14].

The metric for the SDO geometry can be given as

$$ds^2 = \frac{\ell^2}{4}(d\tilde{t}^2 + d\tilde{\psi}^2) + \left(\frac{\tilde{\rho}^2 - \tilde{r}^2}{2}\right) d\tilde{t}d\tilde{\psi} - 4\ell^2 \frac{d\tilde{r}^2}{\tilde{\rho}^2} \tag{2.9a}$$

$$= \ell^2(-r^2 d\tau^2 + \frac{dr^2}{r^2}) + \frac{\ell^2}{4}(d\psi + 2r d\tau)^2 \tag{2.9b}$$

where ψ and $\tilde{\psi}$ are compact direction, $\psi \sim \psi + 2\pi$ and $\tilde{\psi} \sim \tilde{\psi} + 2\pi$, $r \geq 0$ and as before $\tilde{r}^2 +$

$\tilde{\rho}^2 = \ell^2$. As is seen from (2.9b) SDO is an $\mathrm{AdS}_2 \ltimes \mathrm{S}^1$ geometry, with a manifest SL(2,R)×U(1) isometry. The causal boundary of SDO are two disconnected cylinders, the circular section of which is light-like [14]. The SDO in the form (2.9a) and (2.9b) can respectively be obtained from the near horizon limit of near extremal BTZ, and extremal BTZ black holes [15].

3 Unoriented solutions to AdS_3 Einstein gravity

So far we have reviewed the well-established locally AdS_3 solutions. These solutions are obtained by orbifolding AdS_3 by a subgroup of its orientation preserving $SO(2,2)$ isometries. These subgroups, were also chosen such that they preserve the orientation on the $2D$ boundary of the space which has the topology of $R^{1,1}$ or $R^1 \times S^1$. In this section, following [6], we construct all unoriented locally AdS_3 geometries. We classify these geometries, the O-geometries, upon the condition that they have an orientable $2D$ conformal boundary and show that there is an O-geometry for any given orientable class of solutions discussed in previous section.

The orientifold projection we make has a $2D$ fixed surface, the O-surface. One can then distinguish two classes of O-geometries: those with a space-like O-surface which will be discussed in sections 3.1, 3.2 and 3.4, and the other with light-like O-surface to be analyzed in sections 3.2, 3.3 and 3.4.

3.1 Orientifolded AdS_3, O-AdS_3

To start we construct O-AdS_3 which is obtained from orientifolding AdS_3 by a specific $\mathbb{Z}_2$ part of its isometries. This $\mathbb{Z}_2$ is most simply demonstrated in terms of the coordinate frame (A.8), acting by exchange of ρ_1 and ρ_2, while keeping χ_i. In terms of coordinates employed in (A.9) or (A.10) the $\mathbb{Z}_2$ is simply changing $\tilde{r}$ and $\tilde{\rho}$. The metric for O-AdS_3 hence takes the form

$$\begin{aligned} ds^2 &= (\tilde{\rho}^2\theta(\tilde{\Phi}) + \tilde{r}^2\theta(-\tilde{\Phi}))d\tilde{t}^2 - \ell^2\frac{d\tilde{r}^2}{\tilde{\rho}^2} + (\tilde{r}^2\theta(\tilde{\Phi}) + \tilde{\rho}^2\theta(-\tilde{\Phi}))d\tilde{\phi}^2 \\ &= (-|\tilde{\Phi}| + \frac{\ell^2}{2})d\tilde{t}^2 + \ell^2\frac{d\tilde{\Phi}^2}{4\tilde{\Phi}^2 - \ell^4} + (|\tilde{\Phi}| + \frac{\ell^2}{2})d\tilde{\phi}^2 \end{aligned} \tag{3.1}$$

in coordinate system (A.13), where $\tilde{\Phi} = \tilde{r}^2 - \ell^2/2$ and $\theta(x)$ is a step-function: it is zero for $x < 0$, is one for $x > 0$ and is $1/2$ for $x = 0$. We note that (3.1) gives the metric for a double cover of O-AdS_3, *i.e.* (3.1) is the metric of O-AdS_3 in the *covering* AdS_3 space.

Since $\tilde{r}^2 + \tilde{\rho}^2 = \ell^2$, this projection has a fixed locus at $\tilde{r} = \tilde{\rho} = \ell/\sqrt{2}$. This fixed locus, the O-surface, in the notations of Appendix A, falls in region II where $\tilde{t}$ and $\tilde{\phi}$ are both space-like and hence O-surface is a $2D$ space-like R^2-plane and is spanned by $\tilde{t}$ and $\tilde{\phi}$. Upon the projection the geometry at the two sides of this O-surface are identified, *i.e.* the O-AdS_3 geometry is defined only in $\tilde{\Phi} \geq 0$ region and considering $\tilde{\Phi} \in R$ is like going to the covering space of the (orientifold) projection. The orientifold fixed plane is where the volume-form of the AdS_3 space shifts sign. As is seen from the metric (3.1) the volume-form for $\tilde{\Phi} > 0$

($\tilde{r}^2 > \tilde{\rho}^2$) region is proportional to $\tilde{r}d\tilde{r}$, while for $\tilde{\Phi} < 0$ ($\tilde{r}^2 < \tilde{\rho}^2$) region to $\tilde{\rho}d\tilde{\rho} = -\tilde{r}d\tilde{r}$, explicitly exhibiting the orientation flip at $\tilde{r}^2 = \tilde{\rho}^2$ point.

It is instructive to study the space-like O-surface from the global AdS_3 viewpoint. Using the coordinate systems introduced in Appendix A, we have

$$\tilde{r}^2 = \tilde{\rho}^2 = \ell^2/2 \quad \Longrightarrow \quad \cos 2\tau = \sin^2\theta \cos 2\psi \ . \tag{3.2}$$

As we see, close to the boundary ($\theta = \pi/2$) this leads to $\tau = \pm\psi + n\pi,\ n \in \mathbb{Z}$ which are light-like directions on the boundary. At the center of AdS_3 ($\theta = 0$) this is a surface extended in ψ direction and sitting at $\tau = n\pi/4,\ n \in \mathbb{Z}$. One can check that this surface is space-like everywhere in the interior of the AdS_3 covering space while becomes light-like at the boundary.

The metric is obviously locally AdS_3 at any point away from the O-surface at $\tilde{\Phi} = 0$ and hence a solution to pure AdS_3 Einstein gravity. By going to the covering space, one may compute the curvature at the fixed O-surface.[2] Metric, by construction, is continuous at the O-surface. The Ricci tensor, however, is not continuous and has a jump. One should then analyze the Israel matching conditions [7]. For the latter we use the formulation developed in [8], which is reviewed in Appendix C, and arrive at

$$\breve{R}_{\mu\nu} = \ell^2 \ diag(1, 0, -1) \ \delta(\tilde{\Phi}) \ , \tag{3.3}$$

in $(\tilde{t}, \tilde{r}, \tilde{\psi})$ frame, for the jump in Ricci tensor.[3] Therefore, to account for the jump (3.3) at the fixed O-surface one may introduce a source $S_{\mu\nu}$ on the right-hand-side of Einstein equations. Noting that $\breve{R}_{\mu\nu}$ is traceless (recall that at $\tilde{\Phi} = 0$ $\tilde{t}\tilde{t}$ and $\tilde{\psi}\tilde{\psi}$ components of the metric are equal) one readily obtains

$$|\alpha| S_{\mu\nu} = \frac{\ell^2}{8\pi G} \ diag(1, 0, -1) \ \delta(\tilde{\Phi}) \ , \qquad |\alpha| = \sqrt{|g^{\mu\nu}\partial_\mu\tilde{\Phi}\partial_\nu\tilde{\Phi}|} = \ell. \tag{3.4}$$

One may associate $S_{\mu\nu}$ to a "space-like orientifold plane" with tension T sitting at $\tilde{\Phi} = 0$, i.e.

$$S_{\mu\nu} = \sqrt{detg_2} \ T \ diag(1, 0, -1) \ \delta(\tilde{\Phi}) \ , \tag{3.5}$$

where $\sqrt{detg_2} = \ell^2/2$ is the determinant of induced metric on the orientifold plane, and

$$T = \frac{1}{4\pi G\ell}. \tag{3.6}$$

It is remarkable that the energy momentum tensor of this orientifold plane (cylinder), $S_{\mu\nu}$, has the following properties

$$S^\mu{}_\mu = 0, \qquad S_{\mu\nu}n^\mu n^\nu = 0, \tag{3.7}$$

where n^μ is the time-like vector normal to the worldvolume of the orientifold plane (cylinder), in our coordinate $\mathbf{n} = \frac{1}{\sqrt{2}}\frac{\partial}{\partial r}$ at the O-surface.

[2] This is somewhat similar to the procedure carried out in [16] for computing the curvature at the tip of an orbifold. This point will be discussed further in section 5.

[3] Note that the Ricci scalar is continuous and does not have a jump.

The space-like orientifold plane we have introduced here, similar to the standard O-planes, is not a dynamical object and is located at the orientifold fixed surface. In our case, unlike the usual O-planes, this fixed surface is space-like. Despite this point, we should stress that the conformal boundary of the O-AdS_3 is still an orientable Lorentizan $2D$ surface. Moreover, unlike usual O-planes and despite the fact that we have associated a tension to the O-surface, it does not curve the space: everywhere away from the O-surface the metric is (locally) AdS_3. The Penrose diagram of O-AdS_3 is the same as the Left figure in Fig.2, except for the fact that the suppressed direction ϕ is now non-compact.

It is interesting to note that the density of jump of the action in the region II on the either sides of the O-surface, i.e. action evaluated in $0 \leq \tilde{r}^2 \leq \ell^2/2$ region minus its value in $\ell^2/2 \leq \tilde{r}^2 \leq \ell^2$, is equal to the tension of the space-like orientifold plane. Explicitly

$$\begin{aligned} \Delta S &= \frac{1}{16\pi G}\left[\int_{\tilde{r}^2=\ell^2/2}^{\tilde{r}^2=\ell^2} dV\ (R+\frac{2}{\ell^2}) - \int_{\tilde{r}^2=0}^{\tilde{r}^2=\ell^2/2} dV\ (R+\frac{2}{\ell^2})\right] = \frac{1}{8\pi G\ell}\int d\tilde{t}d\tilde{\psi} \\ &= \int T\ \sqrt{g_2}\ d\tilde{t}d\tilde{\psi}. \end{aligned} \tag{3.8}$$

One may also read the above equation in a different way: computing the value of the gravity action on the *covering* AdS_3 background (using solution (A.9)) in region II, one would obtain the same result as ΔS in (3.8), which in turn is equal to the tension of the O-surface.

3.2 Orientifolded BTZ black holes, O-BTZ

Noting that the orientifold projection which led to O-AdS_3 commutes with the BTZ black hole generating orbifold (2.1), one may combine the two and construct orientifolded BTZ, O-BTZ, geometries. Explicitly, O-BTZ geometry is obtained by applying the $\mathbb{Z}_2$ projection which in BTZ coordinates of (2.4) takes the form

$$r^2 \longleftrightarrow \rho^2, \tag{3.9}$$

while keeping τ and ϕ, on the BTZ geometry. The double cover of O-BTZ metric (or O-BTZ metric in the covering space) is then

$$ds^2 = [\rho^2\theta(\Phi) + r^2\theta(-\Phi)]d\tau^2 - 8G\ell J d\tau d\phi + [r^2\theta(\Phi) + \rho^2\theta(-\Phi)]d\phi^2 + \frac{r^2dr^2}{16G^2J^2 - \frac{r^2\rho^2}{\ell^2}} \tag{3.10a}$$

$$= (4G\ell^2M - |\Phi|)d\tau^2 - 8G\ell J d\tau d\phi + (4G\ell^2M + |\Phi|)d\phi^2 + \frac{\frac{1}{4}d\Phi^2}{\frac{\Phi^2}{\ell^2} - 16G^2(\ell^2M^2 - J^2)}, \tag{3.10b}$$

where $\theta(X)$ is the step function defined earlier and

$$\Phi = r^2 - 4G\ell^2M = 4G\ell^2M - \rho^2. \tag{3.11}$$

In the coordinate system (3.10) τ and ϕ are both dimensionless. It is apparent that metric (3.10) is invariant under (3.9) which takes Φ to $-\Phi$. (It is useful to note that in terms of Φ the horizons are sitting at $\Phi = \pm 4G\ell\sqrt{\ell^2 M^2 - J^2}$.) The volume element of the geometry is

$$\begin{aligned} dV &= \ell d\tau d\phi \ (\theta(\Phi)\ r dr + \theta(-\Phi)\ \rho d\rho) \\ &= \ell r d\tau d\phi dr \ (\theta(\Phi) - \theta(-\Phi)) = \frac{\ell}{2} d\tau d\phi \ |d\Phi| \ . \end{aligned} \tag{3.12}$$

That is, the two AdS_3 regions on the opposite sides of the dashed line in Fig.2 have opposite orientations.

O-BTZ geometry is defined in $\Phi > 0$ region, where it is locally AdS_3. One would, however, like to study the geometry at the O-surface $\Phi = 0$. With the above choice, metric is clearly continuous at $\Phi = 0$. The jump of the Ricci tensor is

$$\breve{R}_{\mu\nu} = 64G^2(\ell^2 M^2 - J^2)\ diag(1, 0, -1)\ \delta(\Phi) \ , \tag{3.13}$$

in (τ, r, ϕ) frame. This jump is caused by a space-like orientifold plane $\Phi = 0$ with stress tensor $S_{\mu\nu} = T\sqrt{\det g_2}\ diag(1, 0, -1)\ \delta(\Phi)$, where $\det g_2 = 16G^2\ell^2(\ell^2 M^2 - J^2)$ is the determinant of the two dimensional $\tau\phi$ part of metric (3.10) at $\Phi = 0$, and T is given in (3.6). It is notable that the tension T is independent of the the mass M and angular momentum J of the O-BTZ geometry.[4]

The O-BTZ black hole, although does not have inner horizon and the region behind it, has the same line-element as an ordinary BTZ anywhere away from the O-surface. This in particular implies that one may associate a Hawking entropy S_{BH} and temperature T_H to the O-BTZ geometry; S_{BH} and T_H have exactly the same expressions as an ordinary BTZ with the same ADM mass and angular momentum.

Although the above analysis works for extremal as well as non-extremal BTZ cases, the extremal and massless BTZ cases are special in some different ways:

- As depicted in Fig.2 for the extremal ($\ell M = |J|$) case, as well as the massless BTZ case ($\ell M = J = 0$), the O-surface is a light-like cylinder and coincides with the horizon.
- The jump of curvature $\breve{R}_{\mu\nu}$ (3.13) vanishes for the extremal and massless BTZ cases. For these cases there is no need to introduce a stress tensor at the "light-like orientifold plane".

[4]It is instructive to compare our O-BTZ construction and that of (the Lorentzian section of) the geometry constructed in [17]. In the latter, closed time path (CTP) formulation which is often used in real-time non-zero temperature field theory analysis, was applied to the $2d$ CFT's dual to BTZ black holes. The BTZ background was then used as a basis to construct background geometries appropriate for applying gravity dual of CTP formalism. The Lorentizan sector of the geometry discussed in [17] is closely related to our construction in that they cut the BTZ geometry at a constant $r = r_F$ in the region between the two horizons of BTZ black hole (in their case r_F^2 is not necessarily $4GM\ell^2$). In their construction, however, the matching conditions for the geometry is satisfied without any δ-function jump at the junction. This seems to be related to the fact that, due to the CTP formalism, the action on the two sides of the junction should be related by a minus sign. (We note that this is exactly the case for our O-BTZ geometries: the action computed over the $\Phi > 0$ and $\Phi < 0$ regions of the O-BTZ geometry are equal up to the sign, *cf.* the last paragraph of section 3.1.) We would like to thank Kostas Skenderis and Balt van Rees for several clarifying email exchanges on this point.

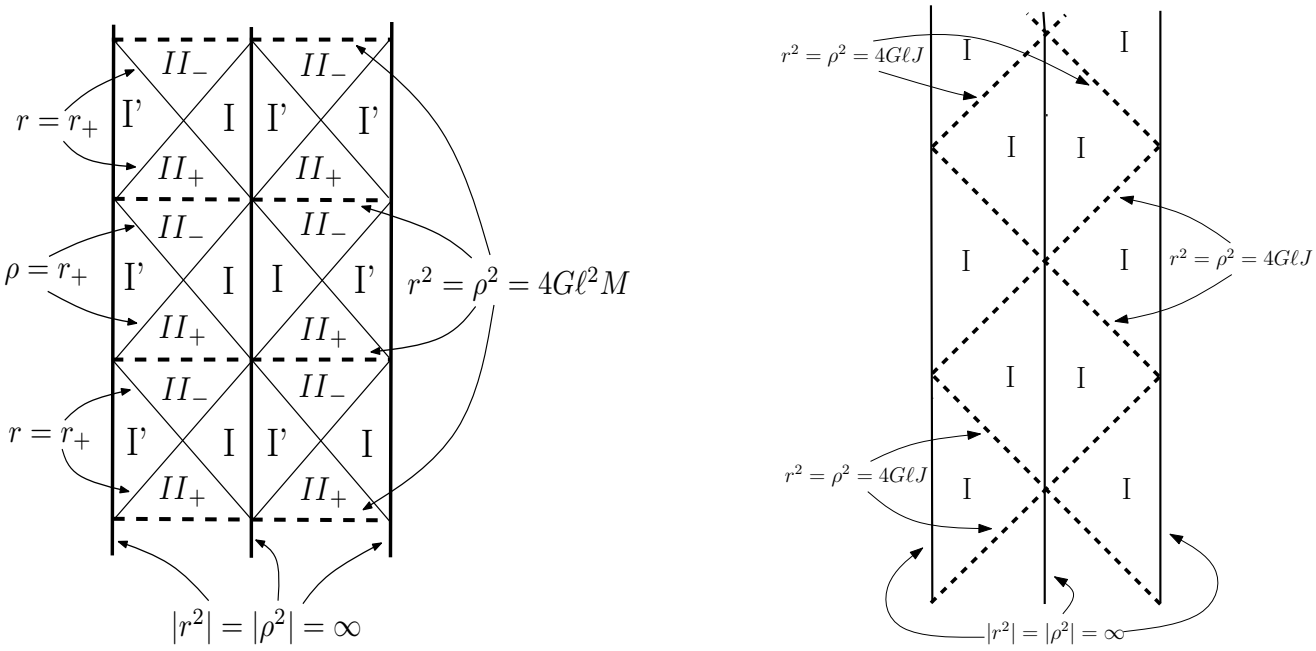

Figure 2: *Two Penrose diagrams of two O-BTZ black holes in the covering space drawn side-by-side.* ***Left figure****: A generic O-BTZ geometry.* The orientifold projection as expected creates a geometry which is the same on the two sides of the orientifold fixed surface, the O-surface. The O-BTZ is then the square part restricted between the two adjacent dashed line. In this sense the Penrose diagram is in fact showing the O-BTZ in the *covering space* of the orientifold projection. In this case the O-surface is a space-like cylinder and is depicted by the horizontal thick dashed line. This space-like cylinder, the circular section of which is suppressed in the Penrose diagram, is located at $r^2 = \rho^2 = 4G\ell^2 M$ and becomes light-like at the boundary. The O-BTZ geometry does not have the region III or "inner horizon" region. The causal boundary of O-BTZ geometry is at $|r^2| = \infty$ which is a cylinder. We point out that the static O-BTZ and a generic (non-extremal) O-BTZ geometries have the same Penrose diagrams. ***Right figure****: An extremal O-BTZ geometry.* The orientifold fixed surface is located at the horizon of the extremal BTZ black hole and, in contrast to the generic O-BTZ case, is hence a light-like surface; a cylinder the circular sections of which is light-like. Again as implied by the orientifolding, and is explicitly seen in the figure, the extremal O-BTZ geometry is the region I, the triangle bounded between two dashed lines and the vertical $r^2 = \infty$ causal boundary, and that the geometry on the other sides of the dashed line are identical. The diagram is showing extremal O-BTZ in its covering space.

- For the extremal case metric is already invariant under the $\mathbb{Z}_2$ (3.9), and one only needs to extend the range of Φ to negative values. As can be seen from the comparison of the Right figures in Figs.1, 2, the only difference between extremal BTZ and extremal O-BTZ is that in the orientifolded geometry there is no need to cut the shaded region (associated with the CTC's).

- Penrose diagram of massless O-BTZ is the same as a generic extremal O-BTZ, as depicted in the Right figure in Fig.2. This is in contrast with the Penrose diagram of massless BTZ case, which is just a triangle (see figure 5 of [3]), and is different than that of extremal BTZ. Nonetheless, note that Penrose diagrams of massive BTZ and massless O-BTZ are the same.

Finally we comment that, as in the usual BTZ case, one may still orbifold the O-BTZ geometry by a $\mathbb{Z}_k$, corresponding to reducing the range of ϕ coordinate to $\phi \in [0, 2\pi/k]$. One can readily show that the $\mathbb{Z}_k$ orbifolded BTZ black hole of mass M and angular momentum J is equivalent to a BTZ black hole (without orbifolding) of mass M/k^2 and J/k^2. This result is obviously also true for O-BTZ.

3.3 O-P-AdS$_3$: Orientifolding AdS$_3$ on its Poincaré horizon

A modified version of the orientifold projection applied to AdS$_3$ (*cf.* section 3.1) may be applied to AdS$_3$ in Poincaré coordinates, given by the metric (A.6). This geometry in a similar way can be extended to beyond the Poincaré horizon, $u^2 > 0$ region, by replacing u^2 with $|u^2|$. The metric for the O-Poincaré-AdS$_3$ in its covering space is then

$$ds^2 = \ell^2 \left[|u^2|(-dt^2 + dx^2) + \frac{du^2}{u^2} \right] = \begin{cases} \ell^2 u^2(-dt^2 + dx^2) + \ell^2 \frac{du^2}{u^2} & u^2 > 0, \\ \ell^2 u^2(dt^2 - dx^2) + \ell^2 \frac{du^2}{u^2} & u^2 < 0, \end{cases} \tag{3.14}$$

The O-surface which coincides with Poincaré horizon sits at $u = 0$ and is a $2D$ light-like R^2 plane. This geometry is similar to that of massless O-BTZ ($\ell M = J = 0$) case, except for the fact that here x direction (corresponding to ϕ direction there) is non-compact. (In the massless O-BTZ the O-surface is a light-like cylinder.) The Penrose diagram of O-Poincaré AdS$_3$ is hence the same as the Right figure in Fig.2.

One may compute the jump of the Ricci tensor for metric (3.14) to be

$$\breve{R}_{\mu\nu} = 4u^4 \ \delta(u^2) \ diag(1, 0, -1) = 0,$$

in (t, u, x) frame. As a result (3.14) is a solution to Einstein equation.[5] This is again similar to the massless O-BTZ case.

[5] Although $\breve{R}_{\mu\nu}$ vanishes for this case, one may still formally find the stress tensor $S_{\mu\nu}$ which creates this jump. Using formalism of [8] one finds that $S_{\mu\nu} = \frac{\ell}{4\pi G}|u^2| \ \delta(u^2) \ diag(1, 0, -1)$, which is of course zero. Nonetheless, noting that square-root of determinant of t, x part of metric is $\ell^2|u^2|$, the tension for the light-like orientifold plane is $T = 1/(4\pi G\ell)$, which is the same as the O-BTZ cases.

3.4 Orientifolded self dual AdS_3 orbifold, O-SDO geometry

In this section we construct the O-SDO geometry. There are two such possibilities: to have a space-like O-surface or to have light-like O-surface. For the former, it is convenient to start with the SDO metric given in (2.9a) and apply the $\mathbb{Z}_2$ orientifold projection

$$\tilde{r} \longleftrightarrow \tilde{\rho}, \qquad \tilde{t} \to \tilde{t}, \qquad \tilde{\psi} \to \tilde{\psi}. \tag{3.15}$$

The "space-like O-SDO" metric in its covering space is then

$$ds^2 = \begin{cases} \frac{\ell^2}{4}(d\tilde{t}^2 + d\tilde{\psi}^2) + (\frac{\tilde{\rho}^2-\tilde{r}^2}{2})d\tilde{t}d\tilde{\psi} - 4\ell^2\frac{d\tilde{r}^2}{\tilde{\rho}^2}, & r^2 \geq r_*^2 \\ \frac{\ell^2}{4}(d\tilde{t}^2 + d\tilde{\psi}^2) + (\frac{\tilde{r}^2-\tilde{\rho}^2}{2})d\tilde{t}d\tilde{\psi} - 4\ell^2\frac{d\tilde{\rho}^2}{\tilde{r}^2}\ , & r^2 \leq r_*^2 \end{cases} \tag{3.16}$$

where $\tilde{\psi} \sim \tilde{\psi} + 2\pi$ and $r_*^2 = \ell^2/2$. The orientifold fixed surface, which is located at $\tilde{\Phi} = \tilde{r}^2 - \ell^2/2 = 0$, is a space-like cylinder parameterized by $\tilde{t}$ and $\tilde{\psi}$. The jump in the Ricci curvature is

$$\breve{R}_{\tilde{t}\tilde{\psi}} = \frac{\ell^2}{4}\delta(\tilde{\Phi}) \tag{3.17}$$

and all the other components zero. As we see at $\tilde{r} = \tilde{\rho}$ the off-diagonal part of metric vanishes. As a result $\breve{R}_{\mu\nu}$ is traceless and the corresponding energy-momentum tensor $S_{\mu\nu}$ which creates the Ricci jump (3.17) satisfies (3.7). As in O-BTZ case, one may associate this jump to a space-like orientifold cylinder with tension $T = 1/(4\pi G\ell)$.

For the second possibility, the "light-like O-SDO", we start with the metric (2.9b) and extend the geometry to negative r region by an orientifold projection. This leads to

$$ds^2 = \ell^2(-r^2 d\tau^2 + \frac{dr^2}{r^2}) + \frac{\ell^2}{4}(d\psi + 2|r|d\tau)^2\ , \qquad r \in (-\infty, +\infty). \tag{3.18}$$

In this case the O-surface is a light-like cylinder and in this respect is similar to the extremal O-BTZ cases. The jump of the Ricci at $r = 0$, similar to the extremal O-BTZ case, vanishes and there is no need for the introduction of a new source there. The conformal boundary of both of the above constructed O-SDO geometries are two disconnected cylinders with light-like circular sections.

One can show that the metric (for the double cover of) the "space-like O-SDO" (3.16) can be obtained from taking the near horizon limit over *near extremal* O-BTZ black hole (3.10) and that "light-like O-SDO" (3.18) can be obtained from the *extremal* O-BTZ in the near horizon limit. In other words, taking the near horizon limit commutes with the orientifolding.

4 Geodesic motion on O-AdS_3

In this section we study the geodesic motion on (the covering space of) the O-geometries and in particular focus on the behavior of geodesics at the orientifold fixed surface and establish

the geodesic completeness of the O-geometries which is also suggested by the Penrose diagrams Fig.2. To study geodesics on O-AdS$_3$ it turns out to be more convenient to choose $\tilde{\Phi}$ as one of the coordinates, *i.e.*

$$ds^2 = (-|\tilde{\Phi}| + \frac{\ell^2}{2})d\tilde{t}^2 + \ell^2 \frac{d\tilde{\Phi}^2}{4\tilde{\Phi}^2 - \ell^4} + (|\tilde{\Phi}| + \frac{\ell^2}{2})d\tilde{\phi}^2 \tag{4.1}$$

Since the O-AdS$_3$ geometry has translation symmetries along $\tilde{t}$ and $\tilde{\phi}$, the geodesics are labeled by the two quantum numbers E, L associated with these symmetries

$$\dot{\tilde{t}} = \frac{d\tilde{t}}{ds} = \frac{E}{|\tilde{\Phi}| - \frac{\ell^2}{2}}, \qquad \dot{\tilde{\phi}} = \frac{d\tilde{\phi}}{ds} = \frac{L}{|\tilde{\Phi}| + \frac{\ell^2}{2}} , \qquad E, L \geq 0, \tag{4.2}$$

where s is the affine parameter. The geodesic equation then becomes

$$\dot{\tilde{\Phi}}^2 - \frac{4k}{\ell^2}\tilde{\Phi}^2 - 4\frac{|\tilde{\Phi}|}{\ell^2}(E^2 - L^2) - (2E^2 + 2L^2 - k\ell^2) = 0 \tag{4.3}$$

where $k = 0, +1, -1$ respectively for light-like, space-like and time-like geodesics. In what follows we will study them separately.[6]

4.1 Light-like geodesics

For the $k = 0$ case eq.(4.12) reduces to

$$\dot{\tilde{\Phi}}^2 - 4\frac{|\tilde{\Phi}|}{\ell^2}(E^2 - L^2) - 2(E^2 + L^2) = 0 \ . \tag{4.4}$$

The most general solution of the above for $E \neq L$ is

$$\tilde{\Phi} = \sigma B[(s - s_0)^2 - A] \ , \tag{4.5}$$

where σ is the sign of $\tilde{\Phi}$ and

$$B = \frac{1}{\ell^2}(E^2 - L^2) \ , \qquad A = \frac{E^2 + L^2}{2B^2} \ . \tag{4.6}$$

Depending on the sign of $\tilde{\Phi}_0 = \tilde{\Phi}(s = 0)$, $\dot{\tilde{\Phi}}_0 = \dot{\tilde{\Phi}}(s = 0)$ and B there are some different cases which we discuss below:

i) $E^2 > L^2$ and $\tilde{\Phi}_0 \geq 0$, $\dot{\tilde{\Phi}}_0 \geq 0$: The light-ray starts either in region I or II and moves away from the O-surface, toward the AdS$_3$ boundary. In this case the geodesic never crosses $\tilde{\Phi} = 0$ line.

   If $\tilde{\Phi}_0 > \ell^2/2$, it reaches there at finite coordinate time and bounces back. The motion after the bounce is described by the case ii) below. If $\tilde{\Phi}_0 < \ell^2/2$, it starts in region II and will take infinite coordinate time $\tilde{t}$ to pass to region I.

[6] As the general comment we should stress that whenever a geodesic hits the O-surface, and in the notation of the Left figure of Fig.2, moves from II_- region to II_+, it does not leave the O-BTZ geometry; as if it has reentered the geometry in II_+ region in the bottom of the O-BTZ square. In other words, all the II_+ regions of Fig.2 (and similarly for II_-, I and I' regions) are identified.

ii) $E^2 > L^2$ and $\tilde{\Phi}_0 > 0,\ \dot{\tilde{\Phi}}_0 < 0$. The geodesic starts in either region I or II and moves toward the O-surface and reaches there at $s_1 = s_0 - \sqrt{A}$. For $s > s_1$ one should use the $\sigma = -1$ branch and continues off to the boundary at $\tilde{\Phi} = -\infty$. For this case

$$\tilde{\Phi} = \begin{cases} B[(s - s_1 - \sqrt{A})^2 - A] & s \leq s_1 \\ \\ -B[(s - s_1 + \sqrt{A})^2 - A] & s \geq s_1 \end{cases} \tag{4.7}$$

As we see $\ddot{\tilde{\Phi}}$ at $s = s_1$, where the geodesic crossed $\tilde{\Phi} = 0$, changes sign and jumps by $4(E^2 - L^2)/\ell^2$. Recall, however, discussions of footnote 6.

iii) $E^2 > L^2$ and $\tilde{\Phi}_0 < 0,\ \dot{\tilde{\Phi}}_0 < 0$. The geodesic always remains on one side of the O-surface. This case is similar to the case i) and basically the same as what one has on the AdS_3. This is of course expected as the $\tilde{\Phi} < 0$ and $\tilde{\Phi} > 0$ regions are related by oreintifold projection.

iv) $E^2 > L^2$ and $\tilde{\Phi}_0 < 0,\ \dot{\tilde{\Phi}}_0 > 0$. This case is similar to case ii). The geodesic starts in region III or II, moves toward $\tilde{\Phi} = 0$ and passes through where it receives a "kick" and continues toward boundary in region I. (Recall discussions of footnote 6.) Note, however, that it takes infinite coordinate time to reach to $\tilde{\Phi} = \infty$.

v) $E^2 < L^2$ case. The light ray oscillates back and forth with amplitude $A|B|$ and each oscillation happens in period $4\sqrt{A}$. Each time that the ray reaches $\tilde{\Phi} = 0$ receives a kick.

vi) $E^2 = L^2$ case. In this case the geodesic equation does not depend on the sign of $\tilde{\Phi}$ and in general $\tilde{\Phi} = 2L\sigma'(s - s_0)$, where $\sigma' = \pm 1$ determines the sign of initial velocity.

4.2 Time-like geodesics

In this case the geodesic equation becomes

$$\dot{\tilde{\Phi}}^2 + \frac{4}{\ell^2}\tilde{\Phi}^2 - 4\frac{|\tilde{\Phi}|}{\ell^2}(E^2 - L^2) - (2E^2 + 2L^2 + \ell^2) = 0 \tag{4.8}$$

Generic solution to this equation is of the form of $\cos\frac{2}{\ell}s$ or $\sin\frac{2}{\ell}s$, as in the usual AdS_3 case. Therefore, the massive particles which follow these geodesics feel an infinite harmonic oscillator barrier at the boundary and unlike light-like geodesics will not reach there at a finite coordinate time $\tilde{t}$; the massive particles oscillate on paths the amplitude of which depend on their energy.

The general solution to (4.8) is

$$\tilde{\Phi} = A\cos\frac{2}{\ell}(s + s_0') + \sigma B \tag{4.9}$$

where $\sigma = \pm 1$ is the sign of $\tilde{\Phi}$ and

$$B = \frac{E^2 - L^2}{2} \ , \qquad A^2 = (B + \frac{\ell^2}{2})^2 + \ell^2 L^2 \ . \tag{4.10}$$

As we see $|B| \leq |A|$ and hence it is possible that $\tilde{\Phi}$ crosses the $\tilde{\Phi} = 0$ line for generic values of E and L. For this case one may choose the origin of s such that $\tilde{\Phi}(s = 0) = 0$ and without loss of generality choose $A \geq 0$, leading to [7]

$$\tilde{\Phi} = \begin{cases} -2A \sin \frac{s}{\ell} \sin \frac{s+s_0}{\ell} & \tilde{\Phi} \geq 0 \\ \\ -2A \sin \frac{s}{\ell} \sin \frac{s_0 - s}{\ell} & \tilde{\Phi} \leq 0 \end{cases} \tag{4.11}$$

where $A \sin \frac{s_0}{\ell} = \frac{\ell}{2}\sqrt{2(E^2 + L^2) + \ell^2}$ and we have chosen the solution such that $\dot{\tilde{\Phi}}$ is continuous at the O-surface. As we see the second derivative of $\tilde{\Phi}$, $\ddot{\tilde{\Phi}}$, at $s = 0$, similar to the light-like cases, has a jump and changes sign, from $\frac{4B}{\ell^2} = \frac{2(E^2 - L^2)}{\ell^2}$ to minus itself which is the same jump that a light-like geodesic experiences while crossing the O-surface which means it reappears in the region II_+ on the bottom of the O-BTZ square (*cf.* footnote 6.)

From the above one can conclude that, imposing perfectly reflecting boundary conditions at the conformal boundary of the O-AdS_3 geometry all the causal curves can be completely determined by specifying initial conditions on the orientifold surface at $\tilde{\Phi} = 0$. In other words $\tilde{\Phi} = 0$ is a Cauchy surface.

4.3 Space-like geodesics

In this case we should study

$$\dot{\tilde{\Phi}}^2 - \frac{4}{\ell^2}\tilde{\Phi}^2 - 4\frac{|\tilde{\Phi}|}{\ell^2}(E^2 - L^2) - (2E^2 + 2L^2 - \ell^2) = 0 \ . \tag{4.12}$$

Depending on the values of E and L one can recognize two class of solutions

I) cosh-solutions:

$$\tilde{\Phi} = A \cosh \frac{2}{\ell}(s + s_0') - B\sigma \tag{4.13}$$

where $\sigma = \pm 1$ is the sign of $\tilde{\Phi}$ and

$$B = \frac{E^2 - L^2}{2} \ , \qquad A^2 = (B - \frac{\ell^2}{2})^2 - \ell^2 L^2 = (B + \frac{\ell^2}{2})^2 - \ell^2 E^2 \ . \tag{4.14}$$

In order to have cosh-solution one should then have $E \geq L + \ell$ or $E \leq |L - \ell|$.

[7] $\tilde{\Phi}$ as a function of s is periodic and one may wonder if this may cause a problem with closed causal curves. Noting (4.2), however, one can show that $\tilde{\Phi}(t)$ is not periodic.

II) sinh-solutions:

$$\tilde{\Phi} = A \sinh \frac{2}{\ell}(s + s_0') - B\sigma \tag{4.15}$$

where $\sigma = \pm 1$ is the sign of $\tilde{\Phi}$ and

$$B = \frac{E^2 - L^2}{2}\ , \qquad A^2 = \ell^2 L^2 - (B - \frac{\ell^2}{2})^2 = \ell^2 E^2 - (B + \frac{\ell^2}{2})^2. \tag{4.16}$$

sinh-solution, therefore, exist if $|L - \ell| \leq E \leq L + \ell$. In the sinh-solutions $\dot{\tilde{\Phi}}$ and A always have the same sign.

Note that in either of the above solutions sign of A can be positive or negative. Depending on the sign of $\tilde{\Phi}_0 = \tilde{\Phi}(s = 0)$ and B one can recognize some different cases. The solution for $\sigma = +1, -1$ will respectively be called positive and negative branches.

I) cosh-solutions:

i) $B \geq 0$: In this case necessarily $A\tilde{\Phi}_0 \geq 0$. If $|A| \geq B$ $(E + L \leq \ell,\ E^2 + L^2 \leq \ell^2/2)$ the geodesic always remains in the same positive or negative branch that it started, assuming its minimum (maximum, if $\tilde{\Phi}_0 < 0$) value at $|\tilde{\Phi}| = |A| - B$. While if $|A| < B$ $(E^2 + L^2 \geq \ell^2/2)$ the geodesic moves toward the O-surface at $\tilde{\Phi} = 0$, passes through it and continues toward the boundary at $-\infty$ ($+\infty$ if $\tilde{\Phi}_0 < 0$). Recall, however, footnote 6. In the latter case, after a shift in the origin of s

$$\tilde{\Phi} = \begin{cases} 2|A| \sinh \frac{s}{\ell} \sinh \frac{s - s_0}{\ell} & A \cdot s \leq 0 \\ \\ -2|A| \sinh \frac{s}{\ell} \sinh \frac{s + s_0}{\ell} & A \cdot s \geq 0 \end{cases} \tag{4.17}$$

where $A \sinh \frac{s_0}{\ell} = \frac{\ell}{2}\sqrt{2(E^2 + L^2) - \ell^2}$.

ii) $B \leq 0$, $A\tilde{\Phi}_0 \geq 0$: The geodesic remains in the same branch that it started and does not cross the O-surface. In this case the geodesic does not distinguish AdS_3 from O-AdS_3.

iii) $B < 0$, $A\tilde{\Phi}_0 \leq 0$: This case is possible only if $|B| \geq |A|$. The geodesic oscillates around $\tilde{\Phi} = 0$ with frequency $2|s_0|$ where $A \sinh \frac{s_0}{\ell} = \frac{\ell}{2}\sqrt{2(E^2 + L^2) - \ell^2}$ and the amplitude $|B| - |A|$:

$$\tilde{\Phi} = \begin{cases} 2|A| \sinh \frac{x}{\ell} \sinh \frac{s_0 - x}{\ell} & 0 \leq x \leq s_0 \\ \\ 2|A| \sinh \frac{x}{\ell} \sinh \frac{x + s_0}{\ell} & -s_0 \leq x \leq 0 \end{cases} \tag{4.18}$$

where $x = s - 2ns_0,\ n \in \mathbb{Z}$ and we have chosen the origin of s such that $\tilde{\Phi} = 0$ at $s = 0$.

II) sinh-solutions:

i) If $A\tilde{\Phi}_0 > 0$, geodesic always remains in the same branch and does not cross the O-surface before bouncing off the conformal boundary. These geodesics hence cannot distinguish AdS_3 from O-AdS_3.

ii) If $A\tilde{\Phi}_0 \leq 0$, the geodesic then crosses $\tilde{\Phi} = 0$ line once before reaching the conformal boundary at $|\tilde{\Phi}| = \infty$. For this case, after a shift in the origin of s, the geodesic may be given by $\tilde{\Phi} = A \sinh \frac{2s}{\ell}$. This case is similar to the case discussed in (4.17).

As one can directly see from (4.12), regardless of k and for all three time-like, space-like and light-like geodesics, when a geodesic passes through $\tilde{\Phi} = 0$ surface, $\ddot{\tilde{\Phi}}$ changes sign and jumps by $4(E^2 - L^2)/\ell^2$.

Geodesic analysis on the O-BTZ is quite similar to what we have presented above (except for the fact that L is quantized for O-BTZ) and we do not repeat that here. In particular the orientifold surface which for the generic O-BTZ geometry is a space-like cylinder, is a Cauchy surface. For the extremal O-BTZ or massless O-BTZ case, where this cylinder is light-like, it is a Cauchy horizon. These can be readily seen from the Penrose diagrams in Fig.2.

5 Discussion and Summary

In this work, continuing analysis of [6], we have made a classification of O-geometries, the geometries obtained by modding out asymptotic AdS_3 solutions by a certain orientation changing isometry. As discussed, this is the only remaining possibility which completes the set of solutions to AdS_3 Einstein gravity. Our O-geometries are: 1) asymptotically AdS_3 with $R^{1,1}$ or $R^1 \times S^1$ conformal boundary, 2) axisymmetric and stationary and are hence specified with at most two quantum numbers, and 3) the orientation changing projection is performed such that the orientation at the $2D$ conformal boundary is preserved. This latter, which is a natural demand if we are interested in having the possibility of a dual $2D$ CFT description, leaves us with only one choice for the orientifold projection. In other words, with the above three conditions we have exhausted all the possibilities for O-geometries.

The O-geometries can be classified by i) topology of the O-surface, which is either a $2D$ plane or a cylinder and ii) by the fact that it is space-like or light-like. There are therefore, four possibilities which we discussed in detail in section 3. As discussed the O-surface is a Cauchy surface (or Cauchy horizon for the light-like case) and it is sitting behind the horizon (at the horizon for light-like case). Note that as usual we are imposing perfectly reflecting boundary conditions at the conformal boundary.

By construction and as can be explicitly seen from Penrose diagrams in Fig.2 the geometries on the other sides of the O-surface (dashed lines in Fig.2) are exactly the same. This means that in studying physics on the O-geometries one can restrict oneself to only the part of the geometry between the two adjacent O-surfaces (dashed lines). That is, a generic O-BTZ is the square bounded by the conformal boundary and the horizontal dashed lines and extremal O-BTZ is the triangle bounded by the conformal boundary and the 45° dashed lines. This is compatible with the fact that the O-surface is a Cauchy surface for

generic O-BTZ and a Cauchy horizon for extremal O-BTZ. In this viewpoint our space-time is bounded between O-surfaces; this is like the standard picture in presence of orientifold planes. It is also intriguing to note that Penrose diagram of O-BTZ and the "O-BTZ square", is the same as the Penrose diagram of a de Sitter space [18]. This may help with formulating very much sought for dS/CFT correspondence.

For the *space-like O-surface cases* we associated a stress tensor to the O-surface proportional to a delta-function at its location. (As shown for the light-like O-surfaces there is no need to associate a tension to the O-surface.) We would like to stress that despite this, our O-geometries anywhere away from the O-surface remain locally AdS_3. This, in particular, implies that presence of O-surface cannot be found out using local differential geometry tools, like curvature invariants and as such one may treat our O-geometries as solutions to pure AdS_3 Einstein gravity. In this respect the situation is similar to an ordinary orbifold singularity: The $R^2/\mathbb{Z}_k$ orbifold, despite of having an orbifold singularity, say at $r = 0$, has vanishing curvature and as long as curvature invariants are concerned it is a flat space and a vacuum solution of Einstein gravity. One may, however, associate a delta-function curvature to the orbifold geometry [16], where $R = -\frac{1}{\pi}(1 - 1/k)\delta^2(r)$. This could be put in a more formal wording employing classification of space-time singularities given in [19]. The singularity of O-geometries with space-like O-surfaces is a "quasi-regular" singularity and not a curvature singularity. However, there is a novel difference compared to the case of orbifold singularity or the singularity of Misner space [19]: in our O-geometries the orientifold fixed surface is sitting behind the horizon and not reachable (in finite coordinate time) by the observer living on the conformal boundary.

One may wonder if there is a dual CFT_2 description for the O-geometries. This question may be approached from different viewpoints: taking O-AdS_3 as the vacuum state of a possible dual CFT and study O-BTZ as thermal states in this CFT, or viewing orientifolding as a unitary operation in the CFT_2 dual to an AdS_3 and realizing O-geometries as states in the CFT dual to the original AdS_3 background. The above two viewpoints may become equivalent if one can show that the CFT_2 has two, essentially similar, independent sectors. In either case, the existence of a dual CFT_2 may be anticipated as one may repeat the Brown and Henneaux [20] analysis for the O-AdS_3 geometries, almost verbatim, and obtain a Virasoro algebra as its asymptotic symmetry group with the central charge

$$c = \frac{3\ell}{2G}, \tag{5.1}$$

where ℓ is the AdS_3 radius and G is the $3d$ Newton constant.

The notable feature of O-BTZ geometries is that they do not have inner horizon and the region behind it. This in particular, as is also seen from the Penrose diagram Fig.2, implies that O-BTZ geometries, unlike the BTZ, do not have a region with CTC.[8] Moreover, this is interesting recalling the instabilities associated with the presence of inner horizons: One

[8] We comment that a similar idea namely, cutting the region with CTC's and gluing another part to the geometry for removing the CTC problem has been previously discussed, e.g. see [23]. Our idea of orientifolding, despite the similarity in using the matching conditions at the O-surface, is different as in our setting the geometry on the other sides of the O-surface are identified and that the "junction" surface in our case should be viewed as the end point of our O-geometry space-time.

may study quantum field theory on a BTZ background and compute the vacuum expectation value (VEV) of the energy momentum tensor corresponding to vacuum fluctuations of this quantum field. In doing so, one finds that it blows up at the inner horizon or at $r = 0$ in the static BTZ case [9, 10]. The back-reaction of this energy momentum tensor changes the background BTZ geometry and turns it to a geometry with curvature singularity (see Appendix B). One may then adopt the images method discussed in [9, 10, 13] for the O-BTZ. Noting that the BTZ orbifold projection (2.1) commutes with the projection (3.9), one may readily obtain the expression for the VEV of the energy momentum tensor for the quantum fluctuations on O-BTZ background, $\langle T_{\mu\nu}\rangle_{O-BTZ}$. Explicitly, if we denote the VEV for BTZ background by $\langle T_{\mu\nu}(r)\rangle$,

$$\langle T_{\mu\nu}\rangle_{O-BTZ} = \begin{cases} \langle T_{\mu\nu}(r)\rangle \ , & r^2 \geq \rho^2 \\ \\ \langle T_{\mu\nu}(\rho)\rangle \ , & \rho^2 \geq r^2 \end{cases}$$

and therefore $\langle T_{\mu\nu}\rangle_{O-BTZ}$ remains finite everywhere.

In the way of better understanding the O-geometries and their possible dual CFT_2 description one may embed them into a supergravity or string theory setting. The obvious questions is first whether our orientifold projection and the (worldsheet) orientifold projection performed in string theory are the same or not and whether our O-surfaces are directly related to the orientifold planes of string theory. A suggestive feature in this regard is that the tension associated with the O-surface (3.6) is independent of the details of the O-geometry and is only specified by the Newton constant G and AdS_3 radius ℓ and is inversely proportional to their product. After developing the setting one may ask if, similarly to the Maldacena-Ooguri construction [21], string theory on O-AdS_3 is solvable or not. Among the other things string theory setting may lead us to dual CFT_2 description of the O-geometries.

Acknowledgement

M.M.Sh-J. would like to thank the Abdus Salam ICTP for the hospitality where a part of this research was carried out. We would like to thank Kostas Skenderis and Balt van Rees for useful email correspondence.

A AdS_3 in different coordinate systems

AdS_3 is the maximally symmetric Lorentzian $3D$ space with negative constant curvature and is a hyperboloid,

$$-T_1^2 + X_1^2 - T_2^2 + X_2^2 = -\ell^2, \tag{A.1}$$

embedded in a four dimensional space $\mathbb{R}^{(2,2)}$, with metric

$$ds^2 = -dT_1^2 + dX_1^2 - dT_2^2 + dX_2^2. \tag{A.2}$$

Using the above definition one may adopt various coordinate systems for describing the AdS_3 space. Three of such coordinate systems, the global AdS coordinates, the "BTZ-type"

coordinates and the Poincaré patch coordinates are the ones we will be using in this paper. Here we review the three coordinate systems through solving (A.1) and discuss their relation.

Global coordinates

Global AdS_3 coordinates is given by

$$\begin{aligned} T_1 &= \frac{\ell}{\cos\theta}\cos\tau\ , \quad X_1 = \ell\tan\theta\cos\psi \\ T_2 &= \frac{\ell}{\cos\theta}\sin\tau\ , \quad X_2 = \ell\tan\theta\sin\psi \end{aligned} \tag{A.3}$$

where $\theta \in [0, \pi/2)$ is the radial coordinate and $\tau \in (-\infty, +\infty)$ is the global time and $\psi \in (-\infty, +\infty)$ is the space-like direction which is usually suppressed at the level of the Penrose diagram. The AdS_3 metric in this coordinate system is

$$ds^2 = \frac{\ell^2}{\cos\theta^2}\left(-d\tau^2 + d\theta^2 + \sin^2\theta d\psi^2\right) \tag{A.4}$$

The causal boundary of AdS_3 is the two dimensional plane spanned by τ, ψ sitting at $\theta = \pi/2$.

Poincaré coordinates

These coordinates cover half of the global AdS_3 and their embedding is

$$\begin{aligned} X_1 = \ell u x, \qquad T_1 = \ell u t\ , \\ T_2 - X_2 = \ell u, \qquad T_2 + X_2 = \frac{\ell}{u}\left[1 + u^2(x^2 - t^2)\right] \end{aligned} \tag{A.5}$$

where $u \geq 0$ and $x, t \in \mathbb{R}$. Metric in this coordinate system takes the form

$$ds^2 = \ell^2\left[u^2(-dt^2 + dx^2) + \frac{du^2}{u^2}\right]\ . \tag{A.6}$$

The causal boundary is located at $u = \infty$. $u = 0$ is a light-like direction in the global AdS_3 and is the Poincaré horizon. The metric (A.6) is the geometry which appears in the near horizon limit of D1-D5 system [22].

This coordinate system only covers half of the global AdS_3 because $T_2 - X_2 \geq 0$. To cover the other half one may use a similar coordinate system with u replaced by $-u$. These two patches would then overlap at the Poincaré horizon $u = 0$.

BTZ-type coordinates

This is the coordinate system which is appropriate for constructing (non-extremal) BTZ black hole and is given by

$$\rho_i^2 = -T_i^2 + X_i^2, \qquad i = 1, 2, \tag{A.7}$$

where $\rho_1^2 + \rho_2^2 = \ell^2$ which can be solved as

$$\begin{array}{llll} T_i = \sqrt{\rho_i}\cosh\chi_i, & X_i = \sqrt{\rho_i}\sinh\chi_i, & \rho_i > 0, & -\infty < \chi_i < \infty \\ T_i = \sqrt{-\rho_i}\sinh\chi_i, & X_i = \sqrt{-\rho_i}\cosh\chi_i, & \rho_i < 0, & -\infty < \chi_i < \infty. \end{array} \tag{A.8}$$

Depending on the sign of ρ_i, three distinct regions in AdS_3 can be recognized: region I, where $\rho_1 > \ell^2$ and $\rho_2 < 0$, region II, where $0 < \rho_i < \ell^2$, $i = 1, 2$, and region III, where $\rho_2 > \ell^2$ while $\rho_1 < 0$. Defining $\tilde{\phi} \equiv \chi_1$ and $\tilde{t} \equiv \chi_2$, one verifies that in the region I, the Killing vectors $\partial_{\tilde{t}}$ and $\partial_{\tilde{\phi}}$ are time-like and space-like respectively, while they are space-like and time-like in region III. In region II, both of these Killing vectors are space-like.

In regions I and II, defining $\sqrt{\rho}_1 = \tilde{r}$, the AdS_3 metric becomes

$$ds^2 = (\ell^2 - \tilde{r}^2)d\tilde{t}^2 + \ell^2\frac{d\tilde{r}^2}{\tilde{r}^2 - \ell^2} + \tilde{r}^2 d\tilde{\phi}^2, \tag{A.9}$$

where $\tilde{t} = \chi_1,\ \tilde{\phi} = \chi_2$. For regions II and III $\tilde{\rho} = \sqrt{\rho}_2$ and the metric takes the form

$$ds^2 = \tilde{\rho}^2 d\tilde{t}^2 + \ell^2\frac{d\tilde{\rho}^2}{\tilde{\rho}^2 - \ell^2} + (\ell^2 - \tilde{\rho}^2)d\tilde{\phi}^2. \tag{A.10}$$

Furthermore one can use the identity

$$\tilde{r}^2 + \tilde{\rho}^2 = \ell^2, \tag{A.11}$$

to show that

$$dR^2 \equiv \frac{d\tilde{\rho}^2}{\tilde{\rho}^2 - \ell^2} = \frac{d\tilde{r}^2}{\tilde{r}^2 - \ell^2}. \tag{A.12}$$

So, in region II, the metric can be given by the following line element,

$$ds^2 = \tilde{\rho}^2 d\tilde{t}^2 + dR^2 + \tilde{r}^2 d\tilde{\phi}^2. \tag{A.13}$$

If we extend the $\tilde{r}$ coordinate to region III, where $\tilde{r}^2 < 0$ and similarly extend the $\tilde{\rho}$ coordinate to region I, then the AdS_3 metric in regions I and III can be given by the same line element as (A.13).

B On solutions of AdS_3 Einstein gravity with conformal matter

Here, we solve AdS_3 Einstein equations for the stress tensor which is relevant for studying back reaction of the vacuum expectation value of stress tensor corresponding to vacuum fluctuations of a conformally coupled scalar field theory on static BTZ background, discussed in [9, 10]. Let us, however, consider the more general problem of finding *static* asymptotically AdS_3 geometries coupled to a traceless stress tensor.

Using diffeomorphisms one can always bring any $3D$ static metric to the form

$$ds^2 = -h(r)d\tau^2 + \frac{dr^2}{N(r)} + r^2 d\phi^2, \tag{B.1}$$

where τ assume values in $(-\infty, \infty)$ while ϕ can range over $(-\infty, \infty)$ or can be periodic $\phi \in [0, 2\pi]$ (for the BTZ case). We would like to solve the Einstein field equations

$$R_{\mu\nu} - \frac{1}{2} R g_{\mu\nu} = \frac{1}{\ell^2} g_{\mu\nu} + 8\pi G T_{\mu\nu},$$

in the presence of a traceless energy-momentum tensor

$$T^{\mu}_{\ \nu} = \frac{1}{8\pi G}\ diag(T_1, T_2, -T_1 - T_2), \tag{B.2}$$

where T_1, T_2 are only functions of r, subject to a boundary condition,

$$h(r),\ N(r) \to (r^2/\ell^2) \qquad \text{as} \qquad r \to \infty. \tag{B.3}$$

The three independent field equations are

$$\begin{aligned} &\frac{h'}{h}(T_2 - T_1) + 2(T_2' + \frac{2T_2}{r} + \frac{T_1}{r}) = 0, \\ &N' = 2r(\frac{1}{\ell^2} + T_1), \\ &N\frac{h'}{h} = 2r(\frac{1}{\ell^2} + T_2). \end{aligned} \tag{B.4}$$

To solve the above equations for the four unknowns, $h,\ N,\ T_1,\ T_2$ we need to assume a relation between the variables. We will consider three interesting cases below.

- $T_2 = 0$: One can readily see that equations yield $T_1 = 0$ and $N = h = \frac{r^2}{\ell^2}$.

- $T_1 = 0$: In this case $N = \frac{r^2}{\ell^2} - M$. There are two cases, either $T_2 = 0$ which basically reduces to the previous case or $T_2 \neq 0$ for which $T_2^2 r^4 h = 1$, where M is an integration constant. Replacing $h = r^2 f(r)^2$, then

  $$(\frac{r^2}{\ell^2} - M) f' = \frac{Mf}{r} + \frac{1}{r^2} \tag{B.5}$$

  and $f(r) = 1 + \sum_{n=1} \frac{a_n}{r^n}$. Plugging the f expansion into (B.5) one can compute a_n as a function of M. For the first three coefficients one finds $a_1 = 0$, $a_2 = -\frac{\ell^2 M}{2}$ and $a_3 = -\frac{\ell^2}{3}$. To this order $T_2 = \frac{1}{r^3} - \frac{a_2}{r^5} - \frac{a_3}{r^6} + \cdots$. One can also find a closed form for the solution of (B.5). As it is not illuminating we will not present it here. This solution has curvature singularity at $r = 0$.

- $T_1 = T_2$ which is relevant for the quantum fluctuations mentioned above [9]. The solution for this case is,

  $$T_1 = T_2 = \frac{A}{r^3}, \tag{B.6}$$

  and

  $$N = f = \frac{r^2}{\ell^2} + \frac{2A}{r} - M, \tag{B.7}$$

  where A, M are arbitrary constants. As a result of the back reaction, $r = 0$ in the original static BTZ geometry (which was the orbifold singularity of the BTZ construction) now turns to a curvature singularity.

C Review of matching conditions in Einstein gravity

For completeness we present the refinement of Israel matching conditions [7] developed by Khorrami and Mansouri [8]. Let us suppose that $\Psi = 0$ defines a closed surface in space-time and hence divides the space-time into the inside and outside regions, specified by $\Psi < 0$ and $\Psi > 0$ respectively. Let us denote metric on the other sides of this matching surface by $g^{>}_{\mu\nu}$ and $g^{<}_{\mu\nu}$ and suppose that they are solving Einstein equations in those regions. The metric for the whole space-time is then given by

$$g_{\mu\nu} = g^{>}_{\mu\nu}\ \theta(\Psi) + g^{<}_{\mu\nu}\ \theta(-\Psi) \tag{C.1}$$

Moreover, one can always choose the coordinate system at the junction at $\Psi = 0$ such that

$$g^{>}_{\mu\nu} = g^{<}_{\mu\nu}|_{\Psi=0} \tag{C.2}$$

The question we are now asking is, under which conditions the metric (C.1) is a solution to Einstein equations everywhere. In order to answer this question we need to write down Einstein equations at the junction and for the latter one needs to compute jump in the curvature on the other sides of the junction. One can show that [8]

$$\breve{R}_{\mu\nu} = \left(\frac{1}{2g}[\partial_\mu g]\partial_\nu\Psi - [\Gamma^\rho_{\mu\nu}]\partial_\rho\Psi\right)\delta(\Psi), \tag{C.3}$$

where $[\Gamma^\rho_{\mu\nu}]$ denotes the jump in the Levi-Civita connections, and g is the determinant of the metric. This jump in the curvature should be caused by the stress tensor associated with the junction through Einstein equations at $\Psi = 0$:

$$\breve{R}_{\mu\nu} - \frac{1}{2}\breve{R}g_{\mu\nu} = 8\pi G\breve{T}_{\mu\nu}, \tag{C.4}$$

where $\breve{T}_{\mu\nu} = \alpha S_{\mu\nu}\delta(\Psi)$ and

$$\alpha = \sqrt{|g^{\mu\nu}\partial_\mu\Psi\partial_\nu\Psi|}. \tag{C.5}$$

D O-AdS$_2$

It is possible to orientifold AdS$_2$ too. One may examine orientifolding AdS$_2$ in two different coordinate systems with two different junction conditions. It is straightforward to observe that it is not possible to orientifold AdS$_2$ on its Poincaré horizon. This may be seen recalling that the O-AdS$_2$ in Poincaré patch should have a metric like (3.14) with the dx^2 term dropped. This will make determinant of metric to be discontinuous (to be $+1$ in one side and -1 on the other). We then remain with the second option, which we will discuss below.

The metric is

$$ds^2 = \frac{1}{\ell^2}\left(\rho^2\Theta(\Phi) + r^2\Theta(-\Phi)\right)dt^2 - \ell^2\frac{r^2dr^2}{r^2\rho^2} = \frac{1}{\ell^2}\left(-|\Phi| + \frac{\ell^2}{2}\right)dt^2 + \frac{\ell^2}{4}\frac{d\Phi^2}{\Phi^2 - \frac{\ell^4}{4}}. \tag{D.1}$$

where $\rho^2 = \ell^2 - r^2$ and $\Phi = r^2 - \ell^2/2$ and $\Theta(x)$ is the step function: it is $+1$ when $x > 0$, $1/2$ for $x = 0$ and zero for $x < 0$. The O-surface is hence at $r^2 = \rho^2 \equiv r_*^2 = \ell^2/2$.

We should next examine the Israel matching conditions. Using the formulation developed in [8] one can compute the jump of the Ricci tensor:

$$\breve{R}_{\mu\nu} = diag(1, -4)\ \delta(\Phi)\ . \tag{D.2}$$

Plugging the above into matching condition

$$\breve{R}_{\mu\nu} = 8\pi G \breve{T}_{\mu\nu} = 8\pi G\alpha\ S_{\mu\nu}\delta(\Phi),$$

where $\alpha = \sqrt{|g^{\mu\nu}\partial_\mu\Phi\partial_\nu\Phi|} = \ell$, we get

$$S_{\mu\nu} = \frac{1}{4\pi G\ell}\ diag(1, -4)\ . \tag{D.3}$$

In this case, unlike the AdS_3 cases, $S_{\mu\nu}$ is not traceless. More importantly, we note that this $S_{\mu\nu}$ cannot be associated with a 0+1 dimensional (orientifold) object at constant r (note that $S_{rr} \neq 0$). In this sense the O-AdS_3 and O-AdS_2 are essentially different.

References

[1] E. Witten, "(2+1)-Dimensional Gravity as an Exactly Soluble System," Nucl. Phys. **B311**, 46 (1988).

[2] M. Banados, C. Teitelboim and J. Zanelli, "The Black hole in three-dimensional space-time," Phys. Rev. Lett. **69** 1849 (1992), [arXiv:hep-th/9204099].

[3] M. Banados, M. Henneaux, C. Teitelboim and J. Zanelli, "Geometry of the (2+1) black hole," Phys. Rev. **D48** 1506 (1993), [arXiv:gr-qc/9302012].

[4] S. Carlip, "Quantum Gravity: a Progress Report," Rept. Prog. Phys. **64** 885 (2001), [arXiv:gr-qc/0108040]; "Quantum gravity in 2+1 dimensions," *Cambridge, UK: Univ. Pr. (1998) 276 p.*

[5] O. Coussaert and M. Henneaux, "Self-dual solutions of 2+1 Einstein gravity with a negative cosmological constant," arXiv:hep-th/9407181;

[6] F. Loran and M. M. Sheikh-Jabbari, "O-BTZ: Orientifolded BTZ Black Holes," arXiv:1003.4089 [hep-th].

[7] W. Israel, "Singular hypersurfaces and thin shells in general relativity," Nuovo Cim. B **44S10**, 1 (1966) [Erratum-ibid. B **48** 463 (1967 NUCIA,B44,1.1966)].

[8] R. Mansouri and M. Khorrami, "Equivalence of Darmois-Israel and Distributional-Methods for Thin Shells in General Relativity," J. Math. Phys. **37**, 5672 (1996), [arXiv:gr-qc/9608029].

[9] A. R. Steif, "The Quantum stress tensor in the three-dimensional black hole," Phys. Rev. **D49**, 585 (1994), [arXiv:gr-qc/9308032].

[10] G. Lifschytz and M. Ortiz, "Scalar field quantization on the (2+1)-dimensional black hole background," Phys. Rev. **D49**, 1929 (1994), [arXiv:gr-qc/9310008].

[11] P. Kraus, H. Ooguri and S. Shenker, "Inside the horizon with AdS/CFT," Phys. Rev. **D67**, 124022 (2003). [arXiv:hep-th/0212277].

[12] V. Balasubramanian, T. S. Levi, "Beyond the veil: Inner horizon instability and holography," Phys. Rev. **D70**, 106005 (2004), [arXiv:hep-th/0405048].

[13] C. Krishnan, " Tomograms of spinning black holes," Phys. Rev. **D80**, 126014 (2009), [arXiv:0911.0597[hep-th]].

[14] V. Balasubramanian, A. Naqvi and J. Simon, "A multi-boundary AdS orbifold and DLCQ holography: A universal holographic description of extremal black hole horizons," JHEP **0408**, 023 (2004), [arXiv:hep-th/0311237].

[15] V. Balasubramanian, J. de Boer, M. M. Sheikh-Jabbari and J. Simon, "What is a chiral 2d CFT? And what does it have to do with extremal black holes?," JHEP **1002**, 017 (2010) [arXiv:0906.3272 [hep-th]].

[16] D. V. Fursaev and S. N. Solodukhin, "On The Description Of The Riemannian Geometry In The Presence Of Conical Defects," Phys. Rev. D **52**, 2133 (1995) [arXiv:hep-th/9501127].

[17] K. Skenderis and B. C. van Rees, "Real-time gauge/gravity duality: Prescription, Renormalization and Examples," JHEP **0905**, 085 (2009) [arXiv:0812.2909 [hep-th]].

[18] M. Spradlin, A. Strominger and A. Volovich, "Les Houches lectures on de Sitter space," arXiv:hep-th/0110007.

[19] G. F. R. Ellis and B. G. Schmidt, "Singular space-times," Gen. Rel. Grav. **8**, 915 (1977); "Classification of Singular Space-Times," Gen. Rel. Grav. **10**, 989 (1979).

[20] J. D. Brown and M. Henneaux, "Central Charges in the Canonical Realization of Asymptotic Symmetries: An Example from Three-Dimensional Gravity," Commun. Math. Phys. **104**, 207 (1986).

[21] J. M. Maldacena and H. Ooguri, "Strings in AdS(3) and SL(2,R) WZW model. I, II, III" J. Math. Phys. **42**, 2929 (2001) [arXiv:hep-th/0001053]; J. Math. Phys. **42**, 2961 (2001) [arXiv:hep-th/0005183]; Phys. Rev. D **65**, 106006 (2002) [arXiv:hep-th/0111180].

[22] J. M. Maldacena, "The large N limit of superconformal field theories and supergravity," Adv. Theor. Math. Phys. **2** 231 (1998) [Int. J. Theor. Phys. **38** 1113 (1999)], [arXiv:hep-th/9711200].

P. Kraus, "Lectures on black holes and the AdS(3)/CFT(2) correspondence," Lect. Notes Phys. **755** 193 (2008), [arXiv:hep-th/0609074].

J. R. David, G. Mandal and S. R. Wadia, "Microscopic formulation of black holes in string theory," Phys. Rept. **369** 549 (2002), [arXiv:hep-th/0203048].

[23] N. Drukker, B. Fiol and J. Simon, "Goedel's universe in a supertube shroud," Phys. Rev. Lett. **91**, 231601 (2003). [arXiv:hep-th/0306057].